CHAPTER 3

Phase transitions in novel disulfide-bridged

alkoxycyanobiphenyl dimers

3.1   Introduction

The vast majority of low molar mass liquid crystals are composed of molecules consisting of a single semi-rigid anisometric or mesogenic core attached to which are one or two terminal alkyl chains. In essence, it is the anisotropic interactions between the cores, which give rise to the observation of liquid crystalline behaviour while the alkyl chains tend to reduce the melting point. Indeed for many years it was widely assumed that such a molecular structure was a prerequisite to the observation of liquid crystallinity [1]. It came as a great surprise, therefore, that during the 1980s a wide range of non-conventional molecular structures were shown to support liquid crystallinity [2].

Of all these low molar mass liquid crystals discovered during the 1980s, one class that attracted particular attention and which still remains the focus of much research, are the so-called liquid crystal dimers [3]. Liquid crystal dimers are composed of molecules containing two conventional mesogenic groups linked by a flexible spacer, most commonly an alkyl chain. Thus, liquid crystal dimers contravened the accepted structure-property relationships for low molar mass mesogens by consisting of molecules having a highly flexible core rather than a semi-rigid central unit. In these respect, therefore, these molecules actually represented an inversion of the conventional molecular design for low molar mass mesogens. Griffin and Britt termed this class of materials as Siamese-twins [4]. The first report of such materials was in fact, some 50 years earlier, Vorlander [5] had described liquid crystals having same molecular

architecture as had Rault *et al.* in the mid-1970s [6]. The importance of these two papers had been overlooked, and it was Griffin and Britt's work that catalyzed considerable interest in this class of liquid crystals. Subsequently, several classes of dimeric liquid crystals have been prepared and studied extensively [7-55]. The interest in these materials stems not only from their ability to act as model compounds for liquid crystalline polymers but also from their properties which are quite different from those of conventional low molar mass mesogens [7-55]. In particular, the transitional behaviour of dimers exhibits a dramatic dependence on the length and parity of the flexible spacer in a manner strongly reminiscent to that observed for the polymeric systems.

3.2 Classification of liquid crystal dimers

Dimers can be sub-divided into two broad groups: symmetric dimers in which the two mesogenic units are identical and non-symmetric dimers which contain two different mesogenic moieties. These two groups can be further sub-divided according to the molecular geometry of the mesogenic groups. The various structural possibilities for dimers are shown schematically in figure 1. Dimers in which two identical mesogens are connected *via* a flexible spacer (Figure 1a) are the most widely synthesized and studied mesogens. However, there are now several examples known in which two non-symmetric mesogens are connected (Figure 1b). Figure 1c and 1d represent laterally linked symmetrical and unsymmetrical calamitic dimers. Similar to calamitic systems, symmetric (Figure 1g) and non-symmetric (Figure 1h) discotic dimers are also possible. Linear and lateral calamitic-discotic dimers are represented in Figure 1e and figure 1f. Dimers in which two discogens connected laterally or linearly to a calamitic molecule are depicted in figure 1i and 1j, respectively. In addition to these possibilities, several other

combinations such as, banana-rod, banana-disk and metal-bridged dimers (metallomesogens) and cyclic dimers in which two mesogenic units connected to each other *via* more than one spacer are also possible. These structures have not been shown in figure 1. Further, all the above-mentioned structures are also possible with a rigid spacer instead of a flexible spacer.
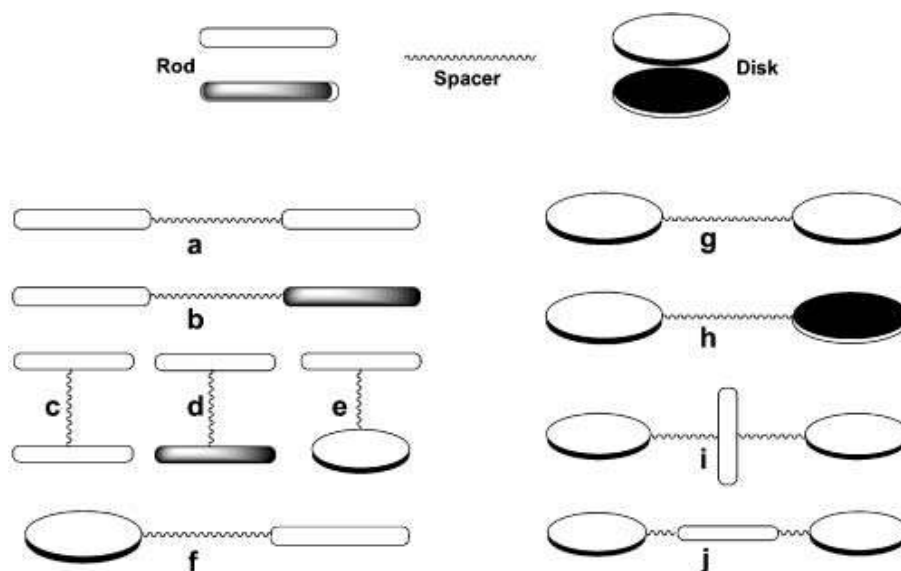

Figure 1. Sketches of some possible molecular architectures for liquid crystal dimers: (a) symmetric calamitic dimer; (b) non-symmetric calamitic dimer; (c) laterally linked symmetric calamitic dimer; (d) laterally linked non-symmetric calamitic dimer; (e) lateral discotic-calamitic dimer; (f) linear discotic-calamitic dimer; (g) symmetric discotic dimer; (h) non-symmetric discotic dimer; (i) two discogens laterally linked to a calamitic molecule; (j) two discogens terminally linked to a calamitic molecule.

3.3   Structure-property relationships in liquid crystal dimers

Dimers containing two mesogenic units show interesting mesomorphic behaviour depending on the length of the spacer and the structure of the linking group. For example, dimesogenic compounds containing an oligosiloxyl group form smectic mesophases regardless of the nature

of the terminal substituent, whereas the same types of compounds having a methylene spacer form only nematic phases [47, 48]. An ether linkage between the mesogenic unit and the central polymethylene spacer usually produces nematogens, whereas an ester linkage induces smectogenic properties in the system [48].

The most extensively studied series of liquid crystal dimers are the α,ω-bis(4'-cyanobiphenyl-4-yloxy)alkanes **(1)** [7, 13, 15, 18, 49-55] and these shall be used to illustrate the characteristic behaviour of nematogenic dimers. Recently this particular series has been extended by luckhurst to include the next 12 homologues *i.e.* up to the spacer containing 24 methylene units and all these are also nematogens [56]. These derivatives with their mesomorphic behaviour are listed in table 1.
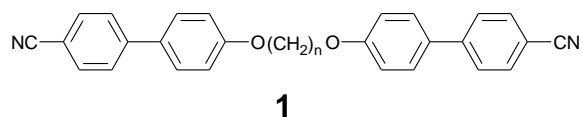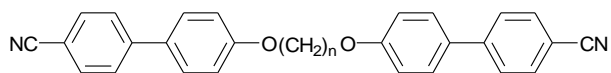

1

Table 1. A list of known alkoxycyanobiphenyl-based calamitic dimers and their thermal behaviour. Cr = crystal, N = nematic phase, I = isotropic. Data in parenthesis (…) denotes a monotropic transition. $\Delta S/R$ = nematic-isotropic transitional entropies as a function of spacer length n.


S.N	n	Thermal behaviour (°C)	$\Delta S/R$	References
1	1	Cr (124) N 144 I	-	18, 56
2	2	Cr 205 N 265 I	1.77	18, 56
3	3	Cr 185 I	0.54	18, 56
4	4	Cr 209 N 250 I	1.95	18, 56

5	5	Cr 137 N 186 I	0.66	18, 56
6	6	Cr 187 N 221 I	1.98	18, 56
7	7	Cr 137 N 181 I	0.78	18, 56
8	8	Cr 175 N 201 I	2.01	18, 56
9	9	Cr 133 N 172 I	0.94	18, 56
10	10	Cr 164 N 184 I	2.14	18, 56
11	11	Cr 124 N 164 I	1.01	18, 56
12	12	Cr 149 N 171 I	2.08	18, 56
13	13	Cr 116 N 152 I	1.06	18, 56
14	14	Cr 152 N 157 I	2.12	18, 56
15	15	Cr 109 N 151 I	1.13	18, 56
16	16	Cr 152 I	2.19	18, 56
17	17	Cr 118 N 145 I	1.23	18, 56
18	18	Cr 147 I	2.18	18, 56
19	19	Cr 125 N 137 I	1.34	18, 56
20	20	Cr 135 I	2.21	18, 56
21	21	Cr 130 I	1.59	18, 56
22	22	Cr 136 I	2.26	18, 56

After that several other symmetric and also non-symmetric dimers have been prepared. The most extensively characterized examples of non-symmetric dimers [57] based on

alkoxycyanobiphenyl as one of the mesogenic units, are the α-(4-cyanobiphenyl-4'-yloxy)-ω-(4-n-alkylanilinebenzylidene-4'-oxy)alkanes **(2).**
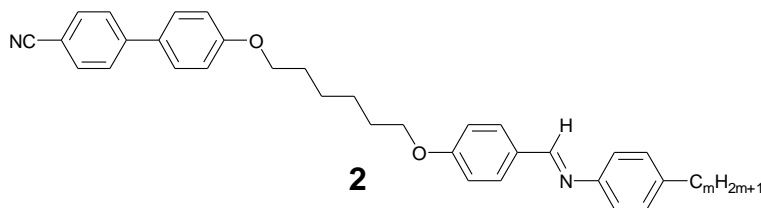

All eleven members in this series were reported to be enantiotropic mesogens and each exhibited a nematic-isotropic transition. T_{N-I} increased markedly on passing from $m = 0$ to $m = 1$ and subsequently decreased as m increased with a small alternation between odd and even members of the series, as observed for conventional low molar mass nematics having high transition temperatures [1]. The thermal behaviour of all the compounds of this series is presented in table 2.

Table 2. A list of known alkoxycyanobiphenyl-based non-symmetric calamitic dimers and their thermal behaviour. Cr = crystal, S_A = smectic A phase, N = nematic phase, S_c = smectic C phase, S = unidentified smectic phase, (….) denotes a monotropic transition. m = no. of carbon atoms in the spacer length.

S. N	m	Thermal behaviour (T/ °C)	References
1	0	Cr 161 S_A (133) N 174 I	57
2	1	Cr 151 S_A (147) N 217 I	57
3	2	Cr 142 S_A 152 N 207 I	57
4	3	Cr 106 S (105) S_A 140 N 210 I	57
5	4	Cr 111 S_A 142 N 202 I	57

6	5	Cr 113 S (87) S_A (109) N 199 I	57
7	6	Cr 116 S_A (95) N 192 I	57
8	7	Cr 116 N 189 I	57
9	8	Cr 119 N 184 I	57
10	9	Cr 116 N 181 I	57
11	10	Cr S_c (103) S_A 155 N 177 I	57

Similarly a number of non-symmetric dimers based on alkoxycyanobiphenyl-pyrene *i.e.* α-(4-cyanobiphenyl-4'-yloxy)-ω-(1-pyreniminebenzylidene-4'oxy)alkanes **(3)** have also been reported [58].


3
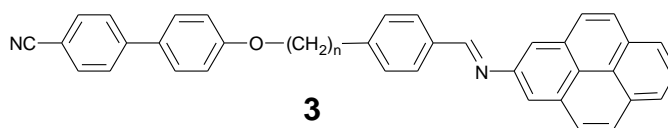
This particular series does not contain a terminal alkyl chain and this clearly strengthens the approximations that the molecules are rigid, cylindrically symmetric particles. The thermal behaviour of all the compounds is listed in table 3.

Table 3. A list of known alkoxycyanobiphenyl-based non-symmetric calamitic dimers and their thermal behaviour. G = glass transition, N = nematic phase, S = smectic phase, [a]data from cooling run, [b]measured using microscope.
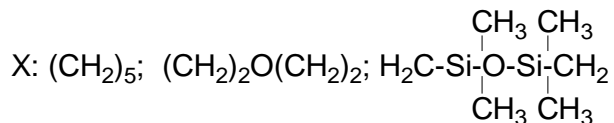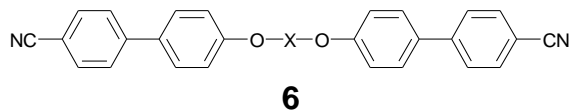
S. N	m	Thermal behaviour	Reference
1	3	G 51 N 120 I	58
2	4	G 54 S 117[a] N 233 I	58

3	5	G 41 S 50 N 154 I	58
4	6	G 41 S 116[a] N 208 I	58
5	7	G 37 S 65 N 164 I	58
6	8	G 33 S 108 N 193 I	58
7	9	G 33 S 55 N 161 I	58
8	10	G 30 S 84[a] N 179 I	58
9	11	G 34 N 159 I	58
10	12	G 29 S 63[b] N 169 I	58

Non symmetric dimers have been prepared in which one mesogenic unit is linked via a terminal position while the other is attached in a lateral position. Weissflog *et al*. [59] synthesized laterally linked cyanobiphenyl based dimers and this exhibits smectic A and nematic phases (**4**). Symmetric and non symmetric chiral liquid crystal dimers [60-65] are also known to exhibits some interesting phases (**5**).
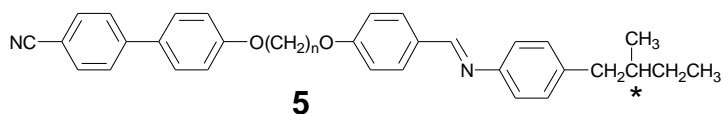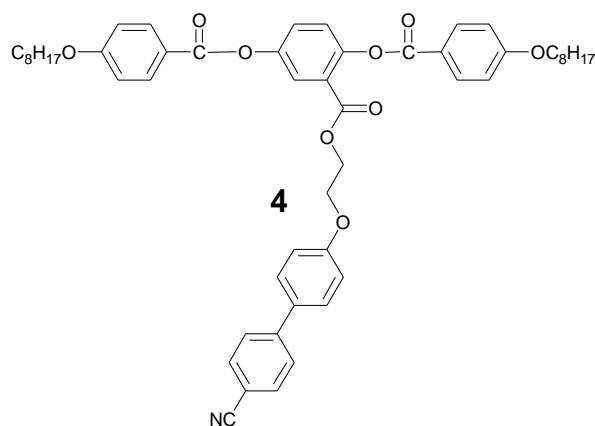
The effects of methylene, ethylene oxide and siloxane spacers on the mesomorphic properties of symmetrical and unsymmetrical liquid crystalline dimers **(6)** containing alkoxycyanobiphenyl have been studied by Creed *et al*. [66].

NC—⬡—⬡—O—X—O—⬡—⬡—CN

6

$$\text{X: } (CH_2)_5; \quad (CH_2)_2O(CH_2)_2; \quad \underset{\underset{CH_3\ CH_3}{|\quad\ |}}{\overset{\overset{CH_3\ CH_3}{|\quad\ |}}{H_2C\text{-Si-O-Si-}CH_2}}$$

It is generally observed that the nematic-isotropic transition temperatures are higher for compounds with an alkoxy chain than for an alkyl chain with the same total number of atoms. This difference is attributed to the higher anisotropy of the molecular polarizability expected for an ether linkage in comparison with a methylene group. Using a molecular field theory for flexible molecules, Emerson and Luckhurst showed that the difference in behaviour between the alkoxy- and alkyl-cyanobiphenyl-based monomers and dimers [67] can be attributed entirely to difference in geometry as shown in figure 2.
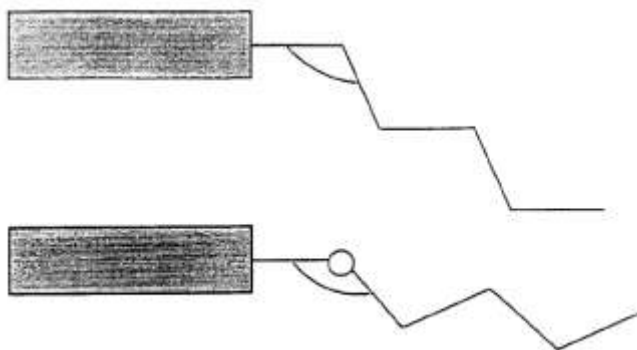

Figure 2. A sketch showing the difference in molecular anisotropy which results when the alkyl chain, in the all *trans* conformation, is linked to a mesogenic group via ether or a methylene group.

120

On the other hand few reports are there of liquid crystal dimers containing discotic mesogeic units and this has been due, in large part, to the difficulties in preparing monofunctionalised discotic precursors. Boden *et al.* reported [68] triphenylene-based dimer **(7)** which exhibits a monotropic discotic hexagonal columnar phase (D$_h$) which can be supercooled to form a glassy D$_h$ phase. Praefcke *et al.* reported a nematogenic discotic dimer **(8)** which was based on two discotic multialkynyl units [69]. Fletcher and Luckhrust attached covalently one disc-like unit and a rod like unit via a flexible spacer yielding a non-symmetric discotic-calamitic liquid crystal dimer **(9)** [70].

7

8

9
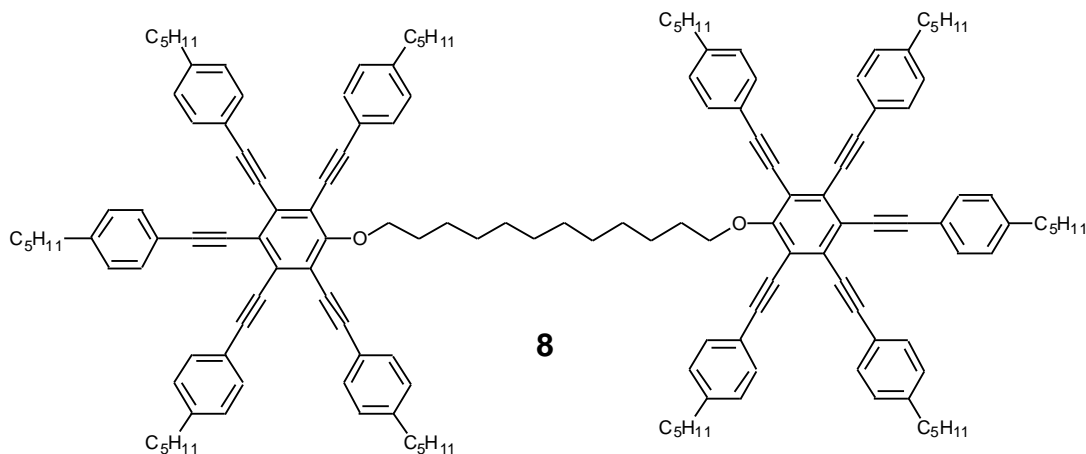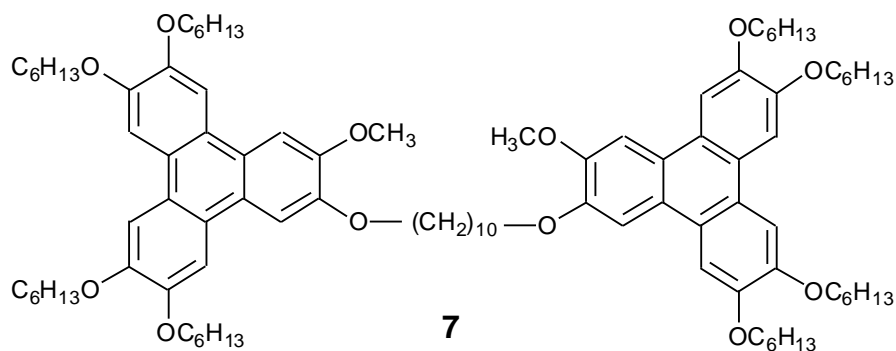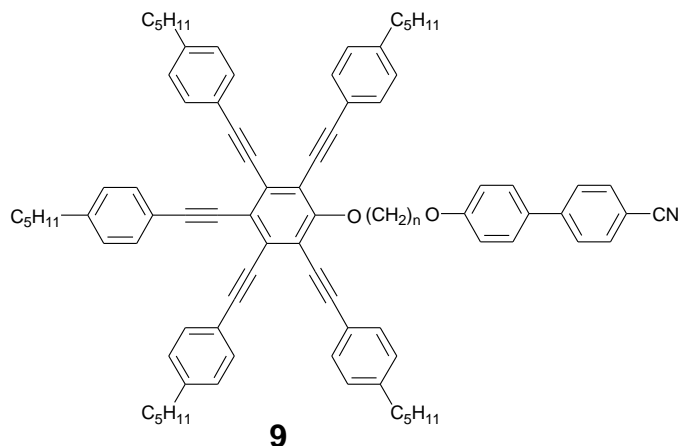
3.4 Objective

The formation of self-assembled monolayers (SAMs) by thiols, disulphides and thioethers on metals, particularly on gold, is well documented. SAMs provide a convenient, flexible and simple system for studies in nanoscience and nanotechnology. A variety of thiols and disulphides have been used to prepare SAMs [71, 72]. A literature survey reveals that while disulphide-bridged discotic dimers have been synshesized **(10)** and used to prepare SAMs [73], calamitic dimesogenic compounds having a disulphide-bridge in the linking unit have not yet been explored.

10
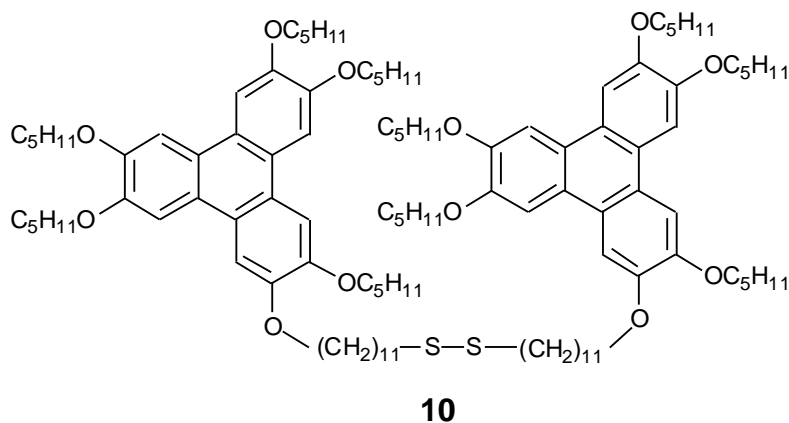
In the case of simple alkoxycyanobiphenyl dimers with a polymethylene spacer, the all *trans* conformation is favoured. There is a large difference in energy between the *cis* and *trans* conformations. The *cis* conformation energy is lower as it requires steric hindrance between two hydrogens in the methylene units. On the other hand, in the case of sulphur-bridged alkoxycyanobiphenyl no hydrogen atom is attached to the sulphur group and thus there will be no steric hindrance. The statistical average of *trans* conformation will be lower in these materials. The geometry and torsional potential of the disulphide group would influence the molecular shape and hence the transition temperatures [67]. As a result the disulfide-bridged dimers will be of particular interest not only to see the effect of transition temperatures but also to compare with the well known alkoxycyanobiphenyl dimers.

In the previous chapter, the synthesis and characterization of mesogenic thiol-functionalized alkoxycyanobiphenyls [74] and their self assembled monolayers on gold [75] has been described. In order to study the effect of sulphur atoms in the linking unit on mesomorphism and SAMs, we have prepared the first examples of disulphide-bridged mesogenic alkoxycyanobiphenyl dimers. The synthesis, characterization and mesomorphic behaviour of these dimers will be discussed in this chapter.

3.5   Synthesis

The synthesis of disulfide-bridged alkoxycyanobiphenyl **15** is outlined in scheme 1. Commercially available 4'-hydroxy-4-biphenylcarbonitrile **11** was alkylated under classical conditions with an excess of the appropriate α,ω-dibromoalkane to obtain the ω-brominated product **12** [76]. The bromo-terminated alkoxycyanobiphenyls **12** were converted to thioacetates **13** by reacting with thioacetic acid. Hydrolysis of the thioacetates furnished the desired thiol-

terminated alkoxycyanobiphenyls **14** which on oxidation with iodine afforded the desired dimers **15**. Detailed experimental procedure has been given in experimental section.
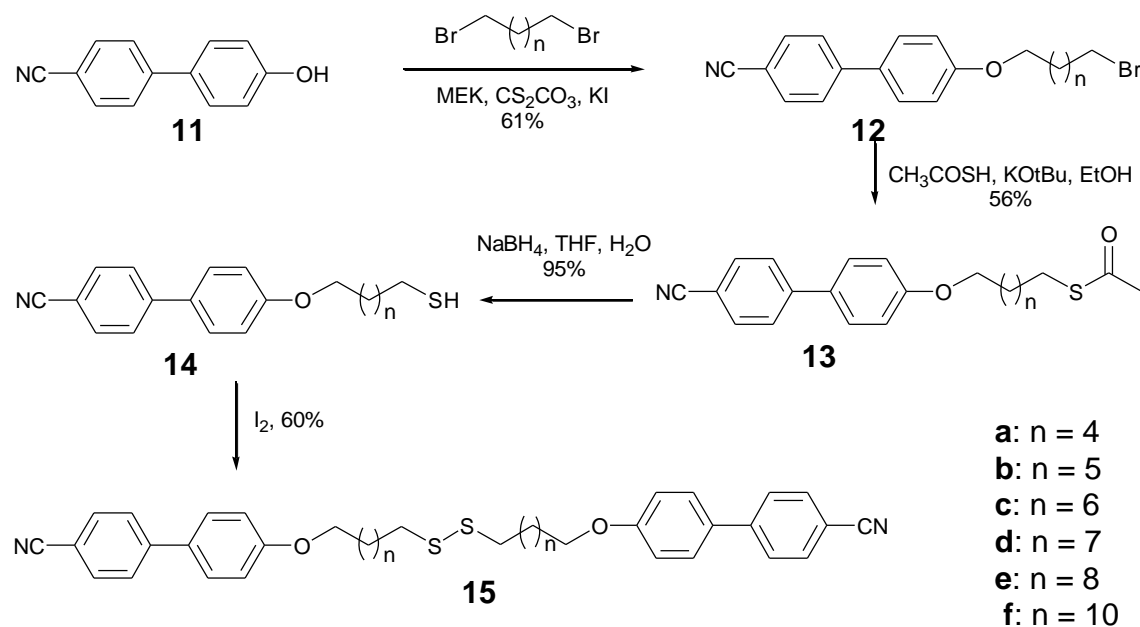

Scheme 1. Synthetic route to disulfide-bridged alkoxycyanobiphenyl dimers.

3.6   Characterization

All the compounds were purified by repeated column chromatography followed by crystallization and characterized from their ^{1}H NMR, ^{13}C NMR, IR, UV spectra and elemental analysis. All the members of the series give similar spectra. Spectral data and elemental analysis of all the compounds were in good agreement with their structures, indicating the high purity of all the materials. Spectral data of all terminally thiol functionalized alkoxycyanobiphenyls are described in chapter 2. Details of the disulphide-bridged dimers spectra are given in experimental section. ^{1}H NMR, ^{13}C NMR, IR, UV-Vis spectra of a few representative members are reproduced in figure 3 to figure 10.

Figure 3 shows   the ^{1}H NMR spectrum of 4'-{[6-({6-[(4'-cyano[1,1'-biphenyl]-4yl)oxy]hexyl}disulfanyl)hexyl]oxy}[1,1'-biphenyl]-4-carbonitrile **(15a)**.

There are four different types of aromatic protons assigned as H_a, H_b, H_c & H_d on the structure given below.
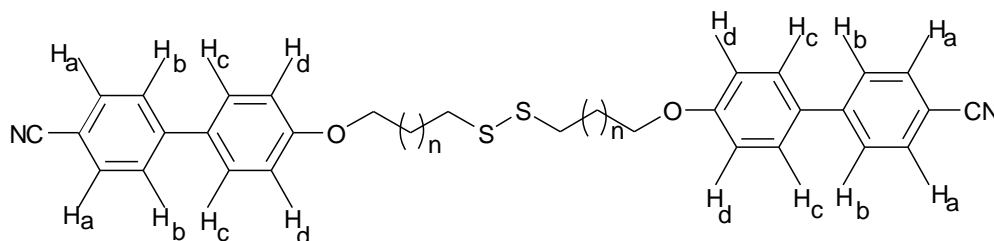
As expected from the above dimer structure, protons which are ortho to –CN group (H_a) are in the same environment and therefore appear at the same δ value. These protons couple with the neighboring H_b protons and appear as doublet (d) and vice-versa. As they are (H_a, H_b) attached to aromatic ring having strongly electron withdrawing –CN group they have δ values higher compare to other hydrogens. Having ortho to –CN group H_a protons will have highest δ values (δ = 7.7) in comparison to H_b protons (δ = 7.6) and obviously, with respect to all other hydrogens. Similarly H_c and H_d protons appear as doublet at δ 7.5 and 6.9 respectively. While Ar-OCH$_2$ appear at δ 4.0 as triplet, -S-CH$_2$ display a triplet at δ 2.7, other aliphatic protons of the chains appear in between δ 1.2 to δ 1.9 as can be clearly seen in the spectrum. This confirms the structure and high purity of the compound. All other derivatives **15b-f** show similar spectrum differing only in the aliphatic protons. The ^{1}H NMR spectrum of compound **15d** and **15f** are reproduced in figure 4 and figure 5, respectively.

Figure 6 represents the ^{13}C NMR spectrum of compound **15a**. Because of the symmetric nature of the molecule it gives only 8 carbon signals (δ 160, 145, 132, 131, 128, 127, 116, 110) for aromatic carbons, one signal for –CN (δ 119), one for –O-CH$_2$ (δ 68), one for –S-CH$_2$ (δ 39) and 4 signals (δ 31, 29, 28, 25) for methylene carbons. All compounds give similar ^{13}C NMR

spectrum differing only in aliphatic carbons. The ^{13}C NMR spectrum of compound **15d** and 1**5f** are reproduced in figure 7 and figure 8.

All the compounds exhibited satisfactory elemental analysis (within +/- 0.4 % of the theoretical values). The elemental analysis data are given in the experimental section.

The IR spectrum of a representative compound **15a** is reproduced in figure 9. It shows expected aromatic and aliphatic stretchings. A strong peak is observed for –CN group at 2200 cm^{-1}.

The UV spectra of all the samples were measured in CH_2Cl_2 and similar spectrum is obtained for all the compounds (**15a-f**). Figure 10 represents the UV-Vis spectrum of the compound **15a**. It shows the absorption peaks at 249 nm.

3.7   Thermal behaviour

All the disulfide-bridged dimers **15a-f** were found to be liquid crystalline. The nature of these liquid crystals was studied by differential scanning calorimetry (DSC) and by optical microscopy with polarized light. Transition temperatures and transition enthalpies were determined by DSC. Data obtained from the heating and cooling cycles of DSC are collected in table 4. The peak temperatures are given in °C and the numbers in the parentheses indicate the transition enthalpy (ΔH) in KJ mol^{-1}.

The lower homologues **15a-d** of the dimer series displayed a distinct nematic phase while smectogenic properties appeared for the higher members (**15e, f**). The first member of the series **15a**, prepared by the dimerization of the terminal thiol **14a** having six methylene units, showed only a monotropic nematic phase. The crystalline compound **15a** melts at 130 ℃ to the isotropic phase. However, on cooling the nematic phase appears at 124 ℃ which crystallizes at 91 ℃. The

DSC traces obtained on the heating and cooling runs are shown in figure 11. Under the microscope it displays a typical schlieren texture of the nematic phase as shown in figure 12.

Table 4. Phase transition temperatures (peak, ºC) and associated enthalpy changes (KJ mol^{-1}, in parentheses) of disulfide-bridged alkoxycyanobiphenyl dimers. Cr: Crystalline phase; N: Nematic phase; SmA: Smectic A phase; I: Isotropic phase.

Compound	Heating scan	Cooling scan
15a	Cr 130.4 (55) I	I 124.2 (3) N 91.2 (44) Cr
15b	Cr 97.2 (49) N 109 (0.5) I	I 108.2 (1.7) N 75 (48) Cr
15c	Cr 107.3 (46.5) N 116 (3) I	I 114 (3.5) N 77.8 (40) Cr
15d	Cr 96.3 (52) N 106.9 (2.5) I	I 105.8 (2.5) N 56.7 (46) Cr
15e	Cr 75.2 (2) Cr 95.8 (70) Sm A 100.2 (0.04) N 108.6 (4) I	I 107.5 (4) N 99.7 (0.04) Sm A 74.7 (55) Cr
15f	Cr 75.5 (3) 82.4 (6) Cr 96.9 (48) Sm A 100.5 (3) I	I 99.6 (6) Sm A 70.5 (44) Cr

The higher homologues **15b** and **15c** exhibits enantiotropic nematic phase. Upon heating, they melt at about 97 ºC and 107 ºC to the nematic phase which clears at about 109 ºC and 116 ºC, respectively. On cooling, the nematic phase appears with only about one degree of super cooling in both the compounds. The compounds crystallize at 75 ºC and 78 ºC respectively on further cooling. The DSC traces and photomicrograph of the nematic texture of compound **15b** and **15c** are shown in figure 13, 14, 15, 16 respectively. Compound **15d** also shows enantiotropic nematic phase. Upon heating it melts at about 96 ºC to the nematic phase which clears at about 107 ºC.

On cooling, the nematic phase appears at 106 ℃ which crystallizes at 57 ℃. The DSC trace of compound **15d** is shown in figure 17. Although its DSC trace shows only a single isotropic-nematic transition at 106 ℃, POM reveals two other second order transitions. On cooling, the appearance of a SmA phase at 83 ℃ and a reentrant nematic phase at 68 ℃ can be clearly seen under the POM [figure 18 (a), (b), (c), (d)]. Compound **15e** shows both nematic (figure 19) and smectic (figure 20) mesophases. In DSC it shows first a crystal to crystal transition at about 75 ℃, melts at 96 ℃ to Sm A phase which transforms to a nematic phase at about 100 ℃ and finally clears at 109 ℃. On Cooling, the isotropic to nematic phase transition appears at about 108 ℃ and the N-SmA transition at 100 ℃. On continue cooling, the compound crystallizes at 75 ℃. In the 2nd heating run the crystal to crystal transition peak is not discernable. The DSC traces obtained on the heating and cooling runs are shown in figure 21. Compound **15f** melts to SmA phase at 97 ℃ which clears at about 101 ℃. Prior to melting it also displays two crystal to crystal transitions at about 76 ℃ and 82 ℃. On cooling the isotropic phase, the SmA phase appears at 99 ℃ which crystallizes at 70 ℃. The typical focal conic fan texture of the SmA phase exhibited by **15f** on cooling from the isotropic phase is shown in figure 22.

The dependence of the transition temperatures on the number of atoms in the spacer for the thiol dimers is shown in figure 23. It is apparent that both melting points and the nematic-isotropic (N-I) temperatures exhibit a smooth falling tendency with increasing number of atoms in the spacer (except for the molecule having 18 number of atoms in the spacer). The large change in T_{N-I} for the compounds with spacers of 14 and 16 atoms could be due to their different crystal packing densities. Deuterium NMR studies have shown that the order parameter for the methylene groups along the chains varies markedly and particularly, the order parameter of the methylene group at 7th and 8th position in 4-*n*-octyl-4'-cyanobiphenyl differ significantly [77].

In comparison with the well known alkoxycyanobiphenyl dimers, which show only N phases, the present series show both N and SmA phases. The T_{N-I} for the alkoxycyanobiphenyl series with odd and even number of methylene units alternate quite dramatically for short spacers, but for long spacers this alternation has essentially vanished and T_{N-I} simply decreases by a small amount with increasing number of methylene units [56]. Because of the presence of disulphide (-S-S-) bridge, the present series of dimers always posses an even number of atoms in the spacer, though they are derived from odd- and even-numbered precursors. All these dimers adopt more or less co-parallel structure and therefore, as expected, do not display any odd-even effect. The energy-minimized structure of compound **15a** is shown in figure 24. Interestingly, the N-I transitional entropy is significantly smaller for the present series which suggests that the order in the nematic phase is small. This is also clear from X-ray diffraction experiments. Additionally the transition temperatures are much lower in the new compounds and the significant reduction in T_{N-I} from m = 14 to m = 16 is not shown by the alkoxycyanobiphenyl series. Although the majority of symmetrical alkoxycyanobiphenyl dimers contain alkyl spacers, a few examples having different spacers such as diethylene oxide and disiloxane have been reported [66]. The nematic–isotropic transitions of these compounds are at much higher temperatures compared with the present dimers. This could be because of the increasing flexibility of the spacer due to presence of a large number of carbon atoms. A similar effect has been observed in the case of oligoethylene oxide spacer [78].

3.8   X-ray diffraction studies

Diffraction patterns of the N and SmA phases of all the compounds show a diffuse peak in the wide angle region, in a direction normal to that of the magnetic field. It has a spacing of about

0.45 nm and corresponds to the average lateral separation of the molecules in these fluid phases. In the SmA phase of the dimer with the longest spacer (**15f**) a single sharp peak is observed in the small angle region of the diffraction pattern along the field direction, figure 25. It has a spacing of 3.84 nm at 96 °C, which matches very well with the spacing expected from an intercalated structure (figure 26). This peak shifts to 3.60 nm at 100 °C in the SmA phase of **15e**, consistent with the decrease in the length of the spacer. A broad peak at 3.52 nm is observed at 105 °C in the N phase of **15e**, indicating the presence of SmA-like short-range order in this phase (figure 27). Such cybotactic nematics are well known near the N-SmA transition and is related to the small enthalpy changes involved in this phase change.

In compounds **15d**, **15c**, **15b** a broad peak is observed in the N phase, at 3.35, 3.17, 2.95 nm, respectively, which indicates the presence of short range SmA-like order. Interestingly these compounds give an additional broad peak in the small angle region of the diffraction pattern along the field direction, with spacings of 1.34, 1.28, 1.20 nm, respectively (figure 28). These spacings are roughly comparable to the length of the rigid aromatic core of the molecule. In case of **15d** which shows the appearance of a SmA phase at 83 ℃ and reentrant nematic phase at 68 ℃ in POM, we have carried out X-ray diffraction experiments at three temperatures (107 ℃ , 75 ℃ and 65 ℃) to confirm these phases. Interestingly, X-ray diffraction patterns are similar for all these different temperatures with increasing the intensity at 75 ℃ that is in the SmA phase. This is logical as with decreasing temperatures the N phase becomes more ordered and more viscous. The increase in viscosity in the N phase can be clearly seen under the microscope. Similar experiments have been done with the compound **15b**. Here also we have carried out X-ray diffraction experiments for three temperatures. The increase in intensity from higher

temperature to lower temperature confirms that viscosity of the N phase increases. This has been shown in figure 29.

Table 5. X-ray diffraction data for thiol dimers

Compound	d-spacing in nm (small angle)	d-spacing in nm (wide angle)
15a	1.15	0.45
15b	2.95, 1.20	0.45
15c	3.17, 1.34	0.45
15d	3.35, 1.28	0.45
15e	3.60, 3.52	0.45
15f	3.84	0.45

In the case of **15a** the peaks corresponding to short range SmA like order is absent and only a broad peak at 1.15 nm is observed, figure 30. This is consistent with the observation that the SmA phase is stabilized with increasing spacer length. As the d-spacing in these dimers is significantly larger than the half length of the molecule, a U-shaped conformation was ruled out. The formation of intercalated smectic phases by several symmetric and non-symmetric dimers has been well documented in the literature [21, 24, 60]. Table 5 summarizes the different d-spacing of these dimers obtained from X-ray diffraction experiments.

3.9   Conclusion

We have reported the first examples of alkoxycyanobiphenyl dimers having a disulfide bridge. X-ray diffraction experiments indicate an intercalated structure for SmA phase of the higher

members of the homologous series. The N phases of all, except the compound with the shortest spacer, show the presence of short-range SmA-like order. We have proposed a possible structural model for the mesophase on the basis of X-ray data. A variety of disulfide-linked dimers can now be designed and created using the above methodology. All the disulfide-bridged dimers form stable monolayers on gold surface (SAMs). This is very useful to study the properties of these dimers at the nanoscale.

3.10   Experimental

3.10.1 General information

General experimental conditions have been described in chapter 2.

3.10.2 Synthesis of thiol dimers (15a-f): General procedure

The synthesis of thiol-functionalized cyanobiphenyls **14** is given in Chapter 2.

Compound **14a** was dissolved in dichloromethane and an excess of iodine was added. The resulting mixture was stirred overnight at room temperature. After that it was poured into 5 % solution of sodium thiosulfate and extracted with dichloromethane. The combined organic extracts were washed with distilled water, dried over anhydrous sodium sulfate and evaporated to dryness. It was then passed through a small silica column using 1:1 dichlomethane-pet ether as an eluant to afford **15a** in 60 % yield.

4'-{[6-({6-[(4'-cyano[1,1'-biphenyl]-4yl)oxy]hexyl}disulfanyl)hexyl]oxy}[1,1'-biphenyl]-4-carbonitrile (15a).

¹H NMR (400 MHz, CDCl₃): δ 7.7 (d, *J* = 8.2 Hz, 4H), 7.6 (d, *J* = 8.2 Hz, 4H), 7.5 (d, *J* = 8.6 Hz, 4H), 6.9 (d, *J* = 8.6 Hz, 4H), 4.0 (t, *J* = 6.4 Hz, 4H), 2.7 (t, *J* = 7.2 Hz, 4H), 1.5-1.9 (m, 16H).

¹³C NMR (100 MHz, CDCl₃, all the derivatives **15a-15f** show similar spectrum): δ 159.8, 145, 132.6, 131.4, 128.4, 127.1, 119.0, 115.2, 110.2, 68, 39, 30.8, 29.1, 28.2, 25.7.

Elemental analysis: calculated for $C_{38}H_{40}N_2O_2S_2$, C 73.53, H 6.48, N 4.51, S 10.35 %; found C 73.13, H 6.48, N 4.88, S 10.85 %.

IR data (KBr, all the derivatives **15a-15f** show similar spectrum) ν_{max} 2854.5, 2923.9, 2219.9, 1602.7, 1521.7, 1602.7, 1492, 1463.9, 1377, 1249.8, 1180.4, 1033.8, 831.3 cm⁻¹.

UV-Vis data (CHCl₃, all the derivatives **15a-15f** show similar spectrum): λ_{max} 295.2 nm.

4'-{[7-({7-[(4'-cyano[1,1'-biphenyl]-4yl)oxy]heptyl}disulfanyl)heptyl]oxy}[1,1'-biphenyl]-4-carbonitrile (15b).

¹H NMR (400 MHz, CDCl₃): δ 7.7 (d, *J* = 8.2 Hz, 4H), 7.6 (d, *J* = 8.2 Hz, 4H), 7.5 (d, *J* = 8.6 Hz, 4H), 6.9 (d, *J* = 8.6 Hz, 4H), 4.0 (t, *J* = 6.4 Hz, 4H), 2.7 (t, *J* = 7.2 Hz, 4H), 1.2-1.8 (m, 20H).

Elemental analysis: calculated for $C_{40}H_{44}N_2O_2S_2$ C 74.05, H 6.82, N 4.31, S 9.87 %; found C 73.74, H 7.1, N 4.67, S 9.5 %.

4'-{[7-({7-[(4'-cyano[1,1'-biphenyl]-4yl)oxy]octyl}disulfanyl)octyl]oxy}[1,1'-biphenyl]-4-carbonitrile (15c).

¹H NMR (400 MHz, CDCl₃): δ 7.7 (d, *J* = 8.2 Hz, 4H), 7.6 (d, *J* = 8.2 Hz, 4H), 7.5 (d, *J* = 8.6 Hz, 4H), 6.9 (d, *J* = 8.6 Hz, 4H), 4.0 (t, *J* = 6.4 Hz, 4H), 2.7 (t, *J* = 7.2 Hz, 4H), 1.2-1.8 (m, 24H).

Elemental analysis: calculated for $C_{42}H_{48}N_2O_2S_2$ C 74.55, H 7.10, N 4.14, S 9.46 %; found C 74.20, H 7.1, N 4.20, S 9.5 %.

4'-{[9-({9-[(4'-cyano[1,1'-biphenyl]-4yl)oxy]nonyl}disulfanyl)nonyl]oxy}[1,1'-biphenyl]-4-carbonitrile (15d).

¹H NMR (400 MHz, CDCl₃): δ 7.7 (d, *J* = 8.2 Hz, 4H), 7.6 (d, *J* = 8.2 Hz, 4H), 7.5 (d, *J* = 8.7 Hz, 4H), 6.9 (d, *J* = 8.7 Hz, 4H), 4.0 (t, *J* = 6.5 Hz, 4H), 2.7 (t, *J* = 7.3 Hz, 4H), 1.2-1.8 (m, 28H).

Elemental analysis: calculated for $C_{44}H_{52}O_2N_2S_2$, C 74.96, H 7.42, N 3.97, S 9.07 %; found C 74.6, H 7.53, N 4.3, S 8.65 %.

4'-{[10-({10-[(4'-cyano[1,1'-biphenyl]-4yl)oxy]decyl}disulfanyl)decyl]oxy}[1,1'-biphenyl]-4-carbonitrile (15e).

¹H NMR (400 MHz, CDCl₃): δ 7.7 (d, *J* = 8.2 Hz, 4H), 7.6 (d, *J* = 8.2 Hz, 4H), 7.5 (d, *J* = 8.7 Hz, 4H), 7.0 (d, *J* = 8.7 Hz, 4H), 4.0 (t, *J* = 6.5 Hz, 4H), 2.7 (t, *J* = 7.3 Hz, 4H), 1.2-1.8 (m, 32H).

Elemental analysis: calculated for $C_{46}H_{56}O_2N_2S_2$, C 75.4, H 7.65, N 3.82, S 8.74 %; found C 75.3, H 7.35, N 3.75, S 9.14 %.

4'-{12-({12-[(4'-cyano[1,1'-biphenyl]-4yl)oxy]dodecyl}disulfanyl)dodecyl]oxy}[1,1'-biphenyl]-4-carbonitrile (15f).

^{1}H NMR (400 MHz, CDCl$_3$): δ 7.7 (d, J = 8.2 Hz, 4H), 7.6 (d, J = 8.2 Hz, 4H), 7.5 (d, J = 8.7 Hz, 4H), 7.0 (d, J = 8.7 Hz, 4H), 4.0 (t, J = 6.5 Hz, 4H), 2.7 (t, J = 7.3 Hz, 4H), 1.25-1.8 (m, 40H) .

Elemental analysis: calculated for C$_{50}$H$_{64}$O$_2$N$_2$S$_2$, C 76.09, H 8.19, N 3.54, S 8.12 %; found C 75.82, H 7.84, N 3.04, S 8.09 %.

References

[1]   G. W. Gray, *The Molecular Physics of Liquid Crystals*, G. R. Luckhrust, G. W. Gray (Eds.) Chap. 1. Academic Press, London (1979).

[2]   (a) D. Demus, *Liq. Cryst*., **5**, 75 (1989). (b) C. T. Imrie, *Physical Properties of Liquid Crystals: Nematics*, D. A. Dunmur, A. Fukuda, G. R. Luckhurst (Eds.) Chap 1.3, INSPEC, London (2001).

[3]   C. T. Imrie, G. R. Luckhurst, *Handbook of Liquid crystals,* vol. 2B, D. Demus, J. W. Goodby, G. W. Gray, H. W. Spiess, V. Vill (Eds.), p. 801, Wiley-VCH, Weinheim (1998).

[4]   A. C. Griffin, T. R. Britt, *J. Am. Chem. Soc*., **103**, 4957 (1981).

[5]   D. Vorlander, *Z. Phys. Chem*., **126**, 449 (1927).

[6]   J. Rault, L. Liebert, L. Strzelecki, *Bull. Soc. Chem. Fr*., 1175 (1975).

[7]   Y. Maeda, H. Furuya, A. Abe, *Liq. Cryst*., **21**, 365 (1996).

[8]   D. Bauman, E. Wolarz, E. Bialecka-florjanczyk, *Liq. Cryst*., **26**, 45 (1999).

[9]   L. Melpezzi, S. Bruckner, E. Galbiati, G. R. Luckhurst, *Mol. Cryst. Liq. Cryst*., **195**, 179 (1991).

[10]   P. J. Barnes, A. G. Douglass, S. K. Heeks, G. R. Luckhurst, *Liq. Cryst*., **13**, 603 (1993).

[11]   D. Ionescu, G. R. Luckhurst, D. S. de Sliva, *Liq. Cryst*., **23**, 833 (1997).

[12]   R. N. Shimizu, N. Asakawa, I. Ando, A. Abe, H. Furuya, *Magn. Reso. Chem*., **36**, S195 (1998).

[13]   A. Abe, S. Y. Nam, *Macromolecules*, **28**, 90 (1995).

[14]   D. J. Photinos, Edward T. Samulski, H. Toriuml, *J. Chem. Soc. Faraday Trans*., **88**, 1875 (1992).

[15]   J. W. Emsley, G. R. Luckhurst, G. N. Shilstone, *Molecular Physics*, **53**, 1023 (1984).

[16]   H. Furuya, T. Dries, K. Fuhrmann, A. Abe, M. Ballauff, E. W. Fischer, *Macromolecules,* **23**, 4122 (1990).

[17]   C. T. Imrie, In *Stucture and bonding*, D.M.P Mingos (ed.), vol. 95, p.149, Springer verlag Berlin Heideberg (1999).

[18]   J. W. Emsley, G. R. Luckhurst, G. N. Shilstone, I. Sage, *Mol. Cryst. Liq. Cryst. Lett.*, **102**, 223 (1984).

[19]   R. W. Date, C. T. Imrie, G. R. Luckhurst, J. M. Seddon, *Liq. Cryst*., **12**, 203 (1992).

[20]   R. W. Date, G. R. Luckhurst, M. Shuman, J. M. Seddon, *J. Phys. II Fr*., **5**, 587 (1995).

[21]   C. T. Imrie, P. A. Henderson, *Curr. Opin. Colloid Inter. Sci*., **7**, 298 (2002).

[22]   A. C. Griffin, S. R. Vaidya, *Liq. Cryst*., **3**, 1275 (1988).

[23]   A. E. Blatch, I. D. Fletcher, G. R. Luckhurst, *Liq. Cryst*., **18**, 801 (1995).

[24]   J. Watanabe, H. Komura, T. Niiori, *Liq. Cryst*., **13**, 455 (1993).

[25]   P. A. Henderson, J. M. Seddon, C. T. Imrie, *Liq. Cryst*., **32**, 1499 (2005).

[26]   J. Watanabe, T. Izumi, T. Niori, M. Zennnyoji, Y. Takanishi, H. Takezoe, *Mol. Cryst. Liq. Cryst*., **346**, 77 (2000).

[27]   H. T. Wang, B. L. Bai, P. Zhang, B. H. Long, W. J. Tian. M. Li, *Liq. Cryst*., **33**, 445 (2006).

[28]   G. S. attard, S. Garnett, C. G. Hickman, C. T. Imrie, L. Taylor, *Liq. Cryst*., **7**, 495 (1990).

[29]   T. Ikeda, T. Miyamoto, S. Kurihara, M. Tsukada, S. Tazuke, *Mol. Cryst. Liq. Cryst. B*, **182**, 357 (1990).

[30]   F. G. Tournilhac, L. Bosio, J. Simon, L. M. Blinov, S. V. Yablonsky, *Liq. Cryst*., **14**, 37 (1993).

[31]   F. Tournilhac, L. Bosio, J. F. Nicoud, J. Simon, *Chem. Phys. Lett*., **145**, 452 (1988).

[32]   F. Tournilhac, L. M. Blinov, J. Simon. S. V. Yablonsky, *Nature Lond*., **359**, 621 (1992).

[33]   P. A. C. Gane, A. J. Leadbetter, P. G. Wrighton, *Mol. Cryst. Liq. Cryst*., **66**, 247 (1981).

[34]   J. W. Goodby, I. Nishiyama, A. J. Slaney, C. J. Booth, K. J. Toyne, *Liq. Cryst*., **14**, 37 (1993).

[35]   G. S. Attard, C. T. Imrie, *Liq. Cryst*., **11**, 785 (1992).

[36]   D. Frenkel, B. M. Mulder, *Mol. Phys*., **55**, 1171 (1985).

[37]   E. J. Zarragoicoechea, D. Levesque, J. J. Weiss, *Molec. Phys*., **75**, 989 (1992).

[38]   D. Frenkel, *J. Phys. Chem*., **91**, 4912 (1987).

[39]   D. Frenkel, *J. Phys. Chem*., **91**, 3280 (1988).

[40]   G. R. Luckhurst, C. Zannoni, P. L. Nordio, U. Segre, *Mol. Phys*., **30**, 1345 (1975).

[41]   C. R. J. Counsell, J. W. Emsley, G. R. Luckhurst, H. S. Sachde, *Mol. Phys*., **63**, 33 (1988).

[42]   R. L. Humphries, P. G. James, G. R. Luckhurst, *J. Chem. Soc. Faraday Trans, II*, **68**, 1031 (1972).

[43]   M. A. Cotter, *Mol. Cryst. Liq. Cryst.*, **39**, 173 (1977).

[44]   J. W. Emsley, G. R. Luckhurst, S. W. Smith, *Mol. Phys*., **70**, 967 (1990).

[45]   A. Ferrarini, G. J. Moro, P. L. Nordio, G. R. Luckhurst, *Mol. Phys*., **77**, 1 (1992).

[46]   A. Ferrarini, G. R. Luckhurst, P. L. Nordio, S. I. Roskilly, *J. Chem. Phys*., **100**, 1460 (1994).

[47]   Jim Jung-IL Jin, *Mol. Cryst. Liq. Cryst*., **267**, 249 (1995).

[48]   B. -W. Jo, T. -K. Lim and J. –I. Jin, *Mol. Cryst. Liq. Cryst*., **157**, 57 (1988).

[49]   A. Abe, H. Furuya, *Polym. Bull*., **19**, 403 (1995).

[50]   A. Abe. H. Furuya, R. N. Shimizu, S. Y. Nam, *Macromolecules,* **28**, 96 (1995).

[51]   D. A. Dunmur, M. R. Wilson, *J. Chem. Soc. Faraday Trans II,* **84**, 1109 (1988).

[52]   J. W. Emsley, G. R. Luckhurst, B. A. Timini, *Chem. Phys. Lett*., **114**, 19 (1985).

[53]   D. Ionescu, G. R. Luckhurst, D. S. de Sliva, *Liq. Cryst*., **23**, 6 (1997).

[54]   S. K. Heeks, G. R. Luckhurst, *J. Chem. Soc. Faraday Trans.,* **89**, 3289 (1993).

[55]   L. Malpezzi, S. Bruckner, E. Galbiati, G. Zerbi, G. R. Luckhurst, *Mol. Cryst. Liq. Cryst*., **195**, 179 (1991).

[56]   G. R. Luckhurst, *Liq. Cryst*., **32**, 1335 (2005).

[57]   J. L. Hogan, C. T. Imrie, G. R. Luckhurst, *Liq. Cryst*., **3**, 645 (1988).

[58]   G. S. Attard, C. T. Imrie, F. E. Karasz, *Chem. Mater*., **4**, 1246 (1992).

[59]   W. Weissflog, D. Demus, S. Diele, P. Nitschke, W. Wedler, *Liq. Cryst*., **5**, 111 (1989).

[60]   A. E. Blatch, I. D. Fletcher, G. R. Luckhurst, *J. Mater. Chem*., **7**, 9 (1997).

[61]   K. Shiraishi, K. Kato, K. Sugiyama, *Chem. Lett*., 971 (1990).

[62]   J. Barbera, A. Omenat, J. L. Serrano, *Mol. Cryst. Liq. Cryst.,* **166**, 167 (1989).

[63]   J. Barbera, A. Omenat, J. L. Serrano, *Liq. Cryst*., **5**, 1775 (1989).

[64]   M. Marcos, A. Omenat, J. L. Serrano, *Liq. Cryst*., **13**, 843 (1993).

[65]   G. R. Luckhurst, R. A. Stephens, R. W. Phippen, *Liq. Cryst*., **8**, 451 (1990).

[66]   D. Creed, J. R. D. Gross and S. L. Sullivan, *Mol. Cryst. Liq. Cryst.,* **149**, 185 (1987).

[67]   A. P. J. Emerson, G. R. Luckhrust, *Liq. Cryst*., **10**, 861 (1991).

[68]   N. Boden, R. J Bushby, A. N. Cammidge, P. S. Martin, *J. Mater. Chem*., **5**, 1857, (1995).

[69]   K. Praefcke, B. Kohne, D. Singer, D. Demus, G. Pelzl, S. Diele, *Liq. Cryst*., **7**, 589 (1990).

[70]   I. D. Fletcher, G. R. Luckhurst, *Liq. Cryst*., **18**, 175 (1995).

[71]   X. Li, J. Huskens, D. N. Reinhoudt, *J. Mater. Chem.*, **14**, 2954 (2004).

[72]   J. Christopher Love, L. A. Estroff, J. K. Kriebel, R. G. Nuzzo, G. M. Whitesides, *Chem Rev*., **105**, 1103 (2005).

[73]   H. Schonherr, F. J. B. Kremer, S. Kumar, J. A. Rego, H. Wolf, H. Ringsdorf, M, Jaschke, H. Butt, E. Bamberg, *J. Am. Chem. Soc*., **118**, 13051 (1996).

[74]   S. Kumar, S. K. Pal, *Liq. Cryst*., **32**, 659 (2005).

[75]   V. Ganesh, S. K. Pal, S. Kumar, V. Lakshminarayanan, *J. Colloid & Interface Science*, **296**, 195 (2006).

[76]   G. S. Attard, R. W. Date, C. T. Imrie, G. R. Luckhurst, S. J. Roskilly, J. M. Seddon, L. Taylor, *Liq. Cryst*., **16**, 529 (1994).

[77]   J. W. Emsley, G. R. Luckhurst, C. P. Stockley, *Proc. R. Soc. Lond. A*, **381**, 117 (1982).

[78]   I. Sledzinska, E. Bialecka-Florjanczyk, A. Orzesko, *Eur. Poly. J*., **32**, 1345 (1996).
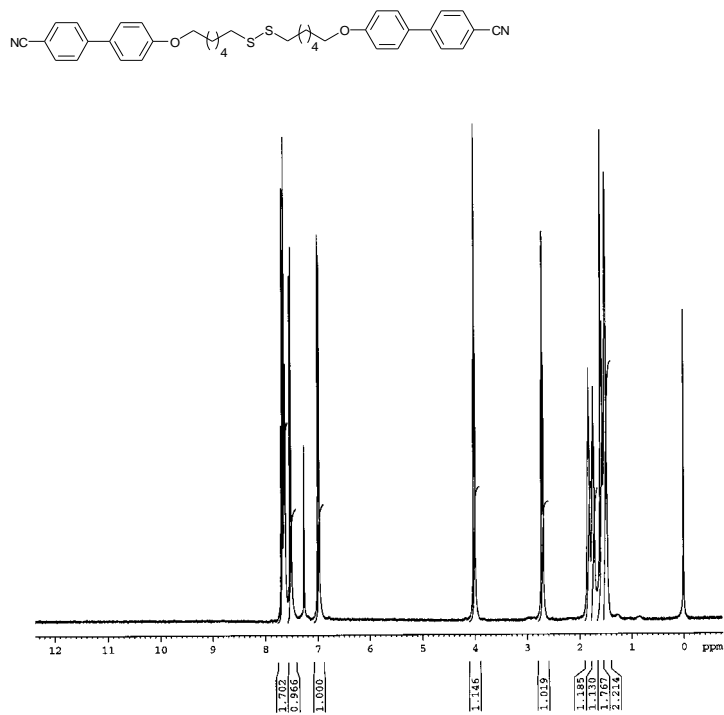
Figure 3. ^{1}H NMR spectrum of the compound **15a**.
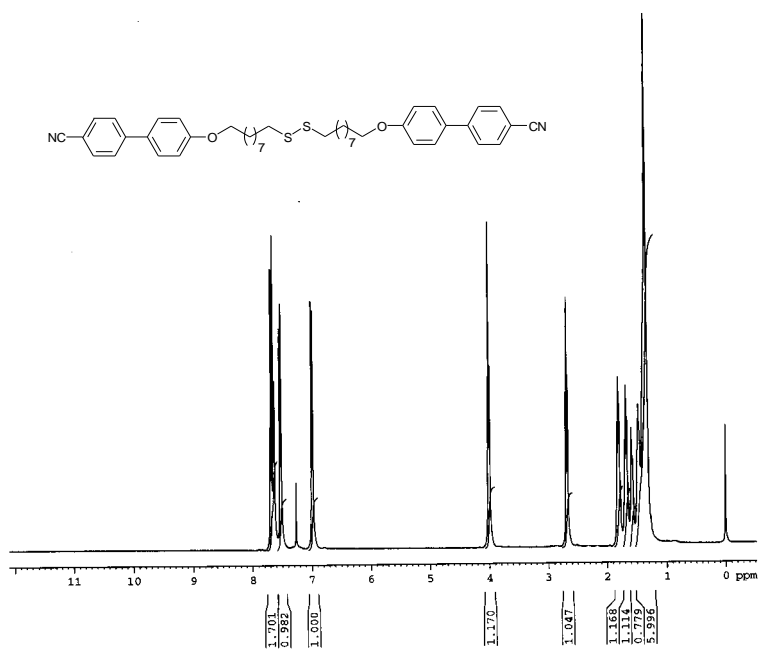
Figure 4. ^{1}H NMR spectrum of the compound **15d**.

141
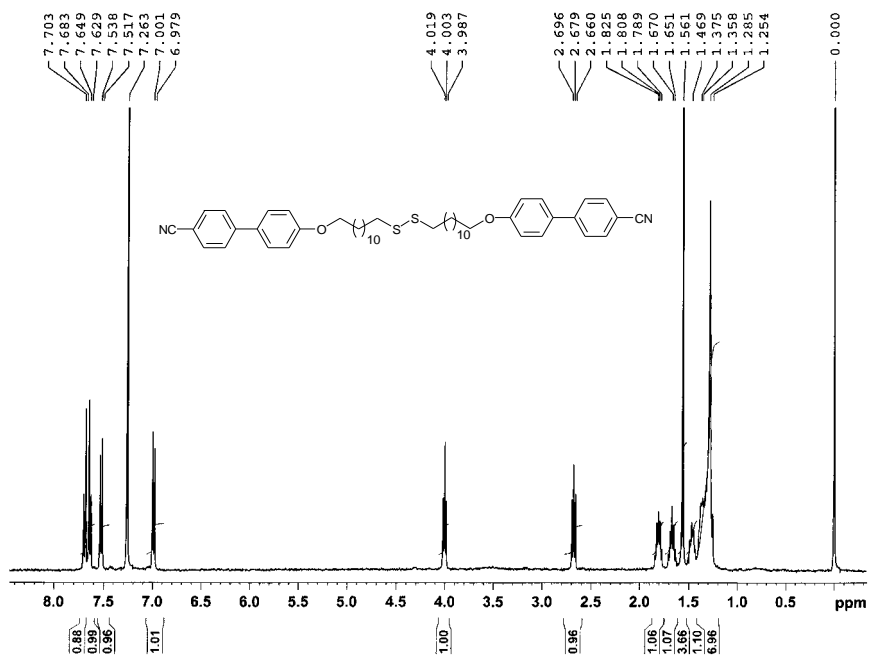
Figure 5. ^{1}H NMR spectrum of the compound **15f**.
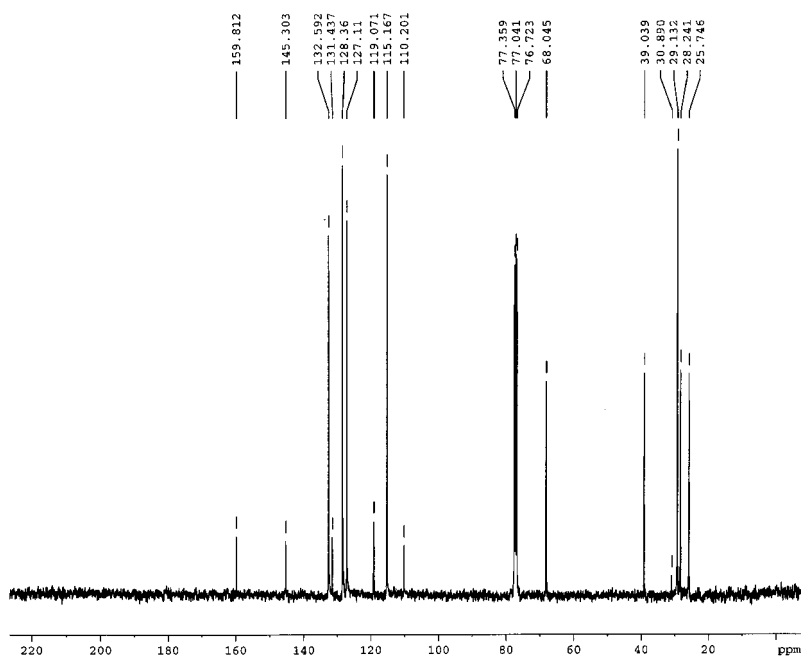
Figure 6. ^{13}C NMR spectrum of the compound **15a**.

142
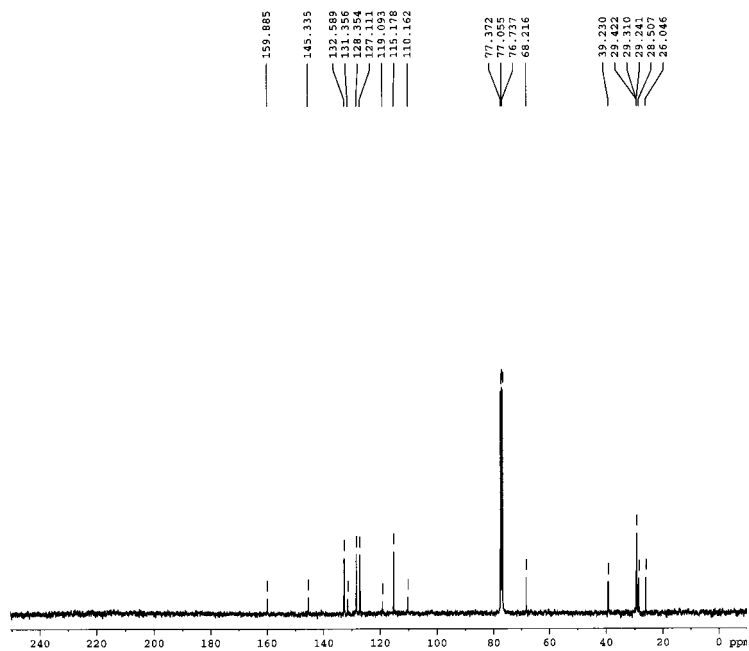
Figure 7. ^{13}C NMR spectrum of the compound **15d**.
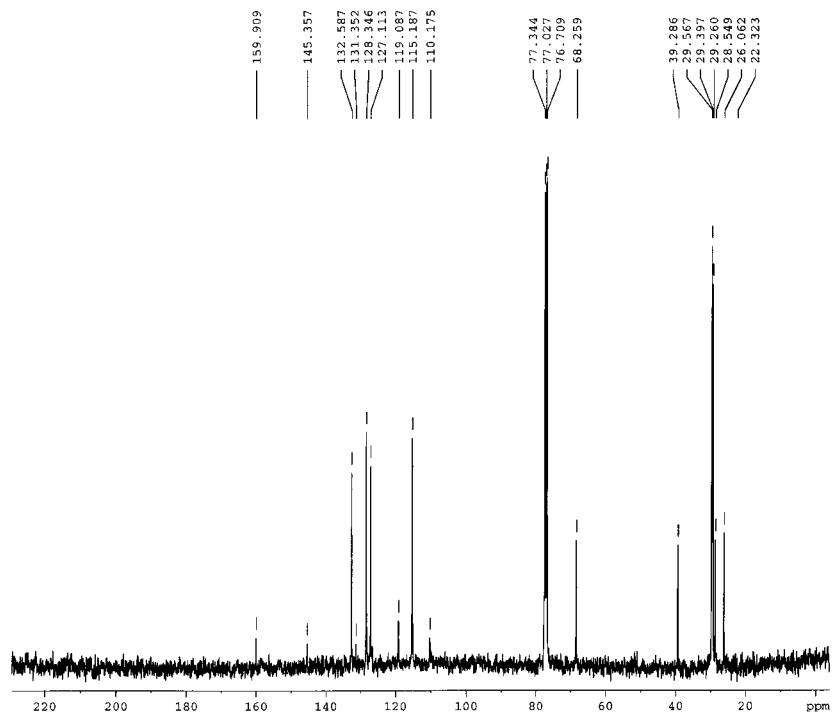
Figure 8. ^{13}C NMR spectrum of the compound **15f**.
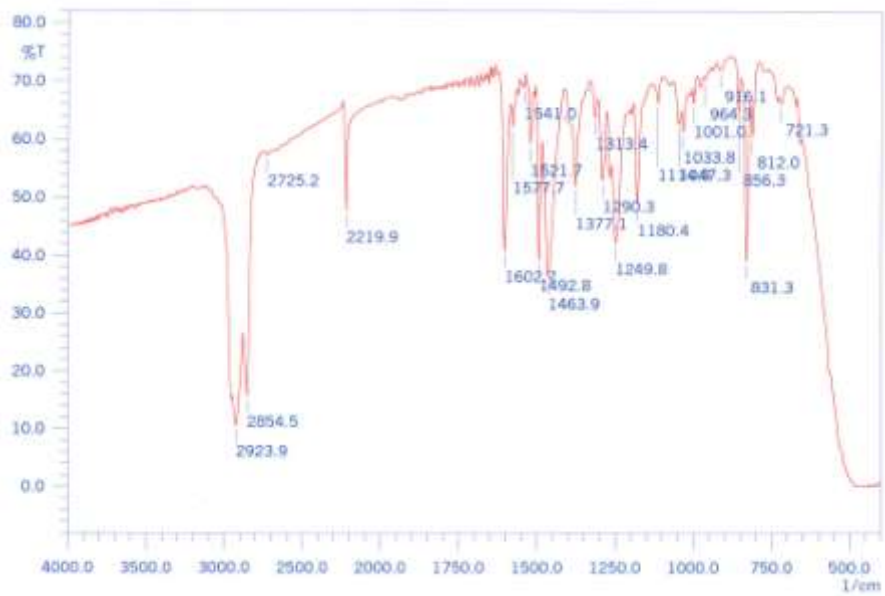
Figure 9. IR spectrum of compound **15a**.
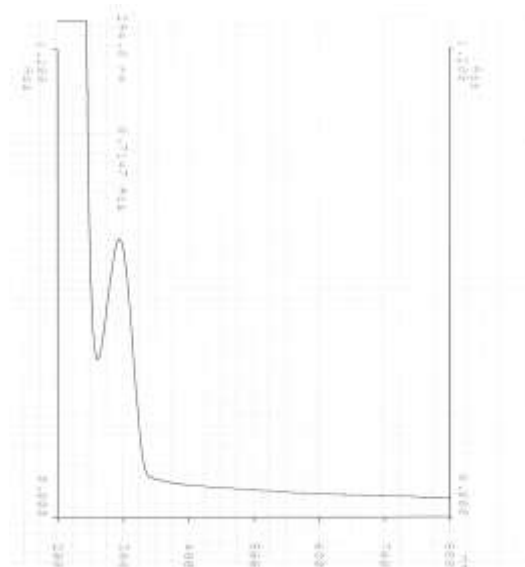
Figure 10. UV spectrum of the compound **15a**.
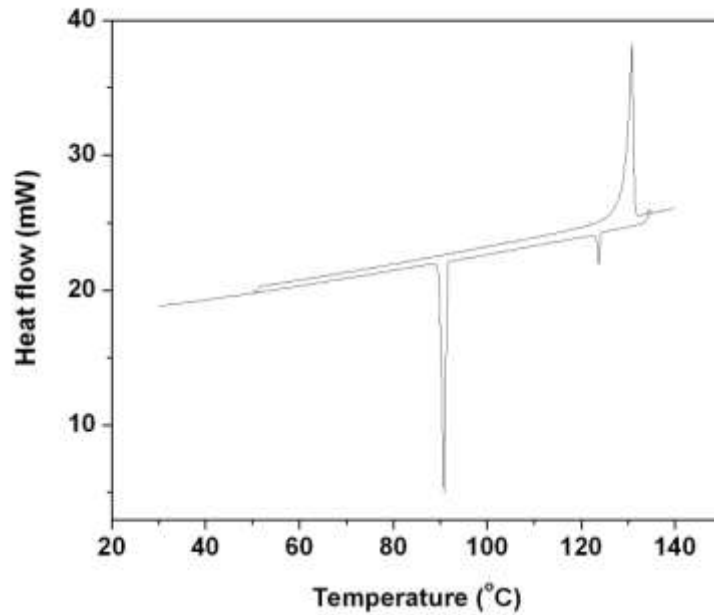
Figure 11. DSC trace of the compound **15a** (scan rate 5 ℃ min[-1]).
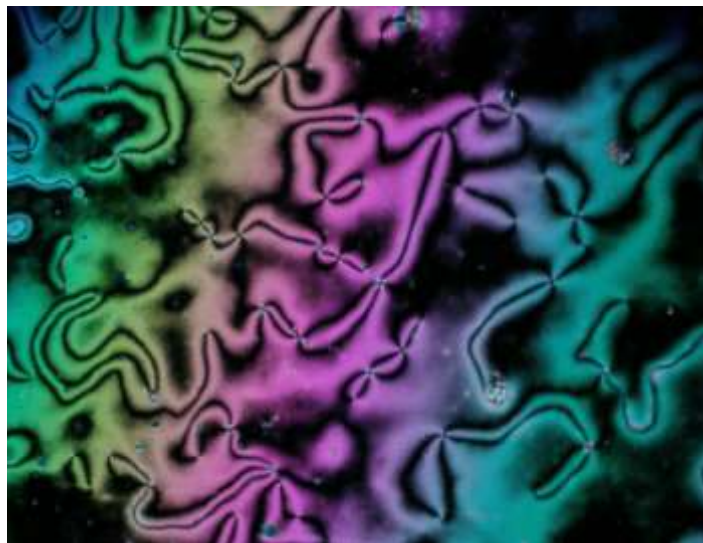
Figure 12. Optical texture of **15a** obtained on cooling from the isotropic liquid at 105 ℃

(crossed polarizers, magnification X 200).
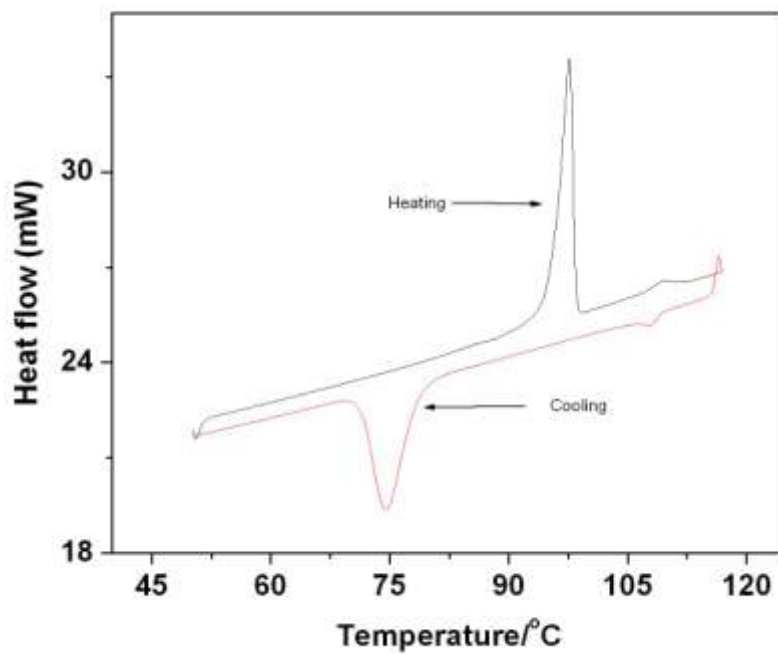
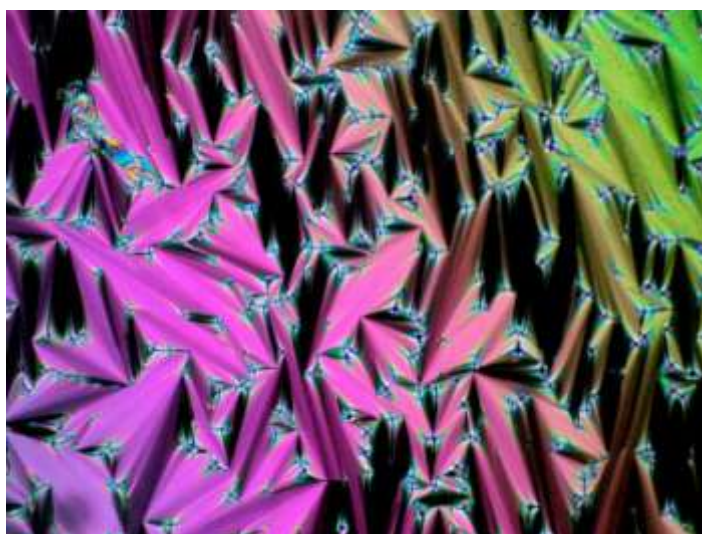**Figure 13**. DSC trace of the compound **15b** (scan rate 5 ºC min⁻¹).
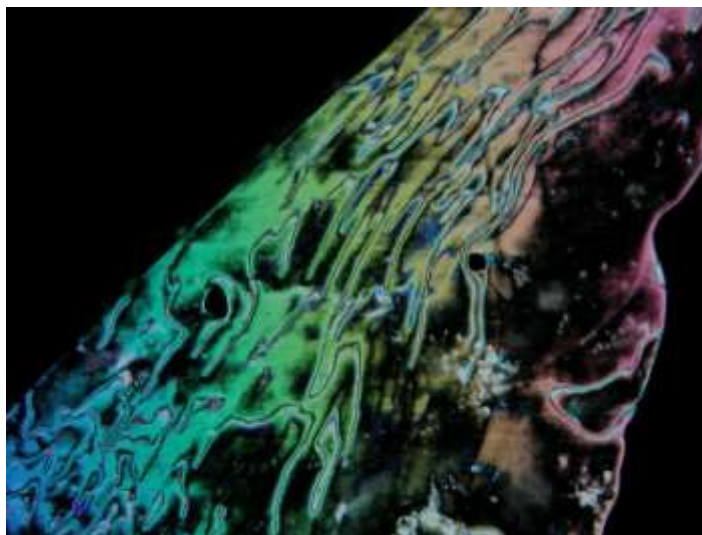
Figure 14. Optical photomicrograph of compound **15b** on cooling the isotropic liquid at 100 ºC

(crossed polarizers, magnification X 200).
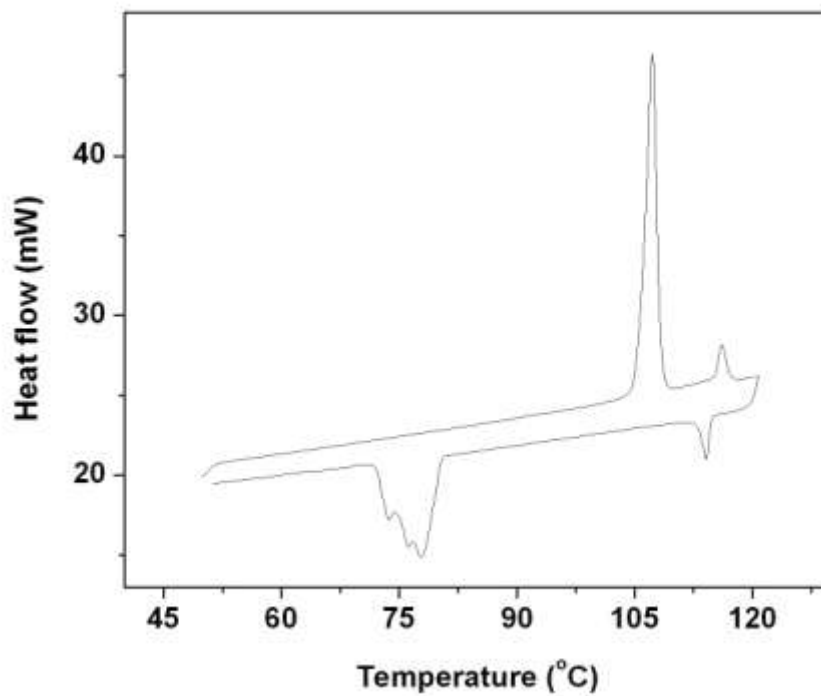
Figure 15. DSC trace of the compound **15c** (scan rate 5 ºC min^{-1}).

Figure 16. Optical photomicrograph of compound **15c** on cooling the isotropic liquid at 100 ºC

(crossed polarizers, magnification X 200).
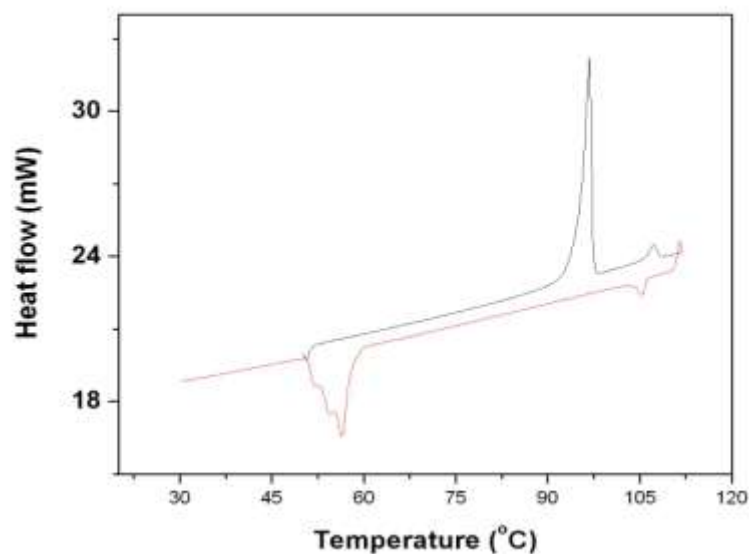
Figure 17. DSC trace of the compound **15d** (scan rate 5 ℃ min-1).

(a)   (b)

(c)   (d)
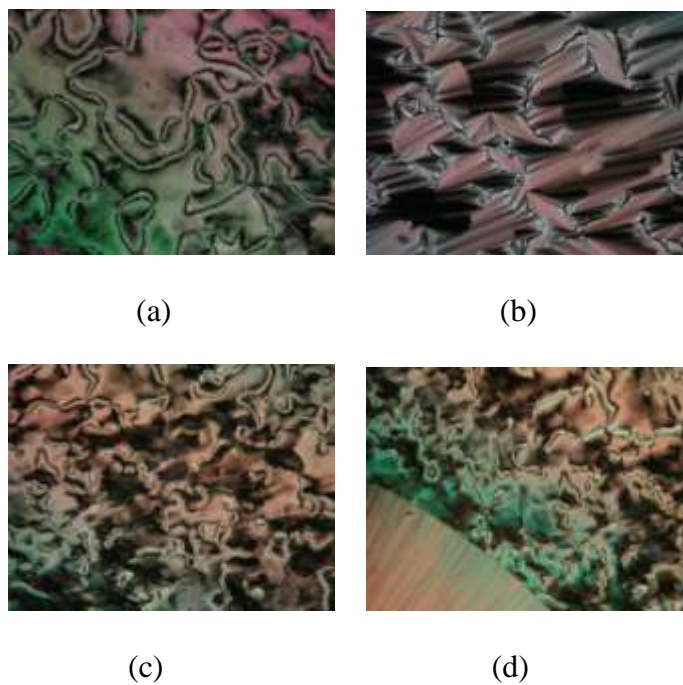
Figure 18. Optical photomicrograph of compound **15d** on cooling from isotropic liquid (a) N phase at 100 °C. (b) SmA phase at 75 °C. (c) reentrant N phase at 68 °C and (d) crystallization starts at 57 °C (crossed polarizers, magnification X 200 for all the photomicrographs).

Figure 19. Optical texture of the nematic phase of dimer **15e** obtained on cooling from the

isotropic liquid at 105 ºC (crossed polarizers, magnification X 200).

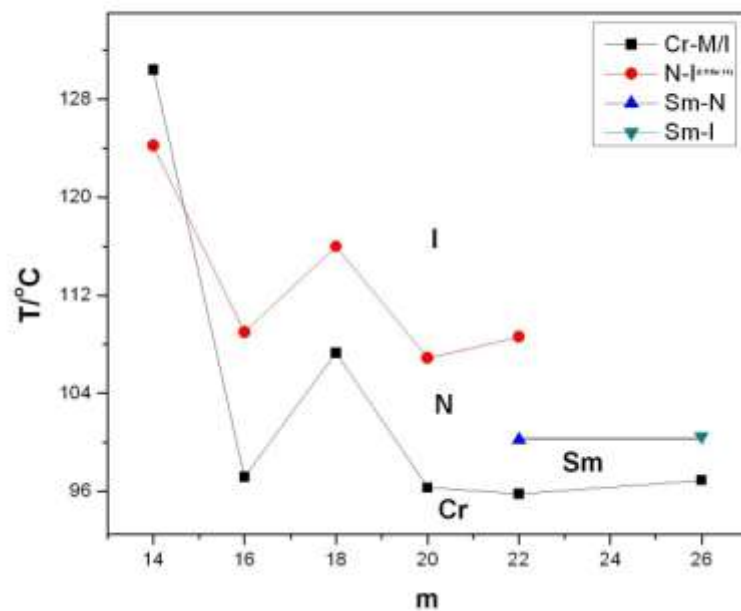**Figure 20**. Focal conic fan textures of SmA phase obtained on slow cooling from the isotropic

liquid of **15e** at 85 ºC.
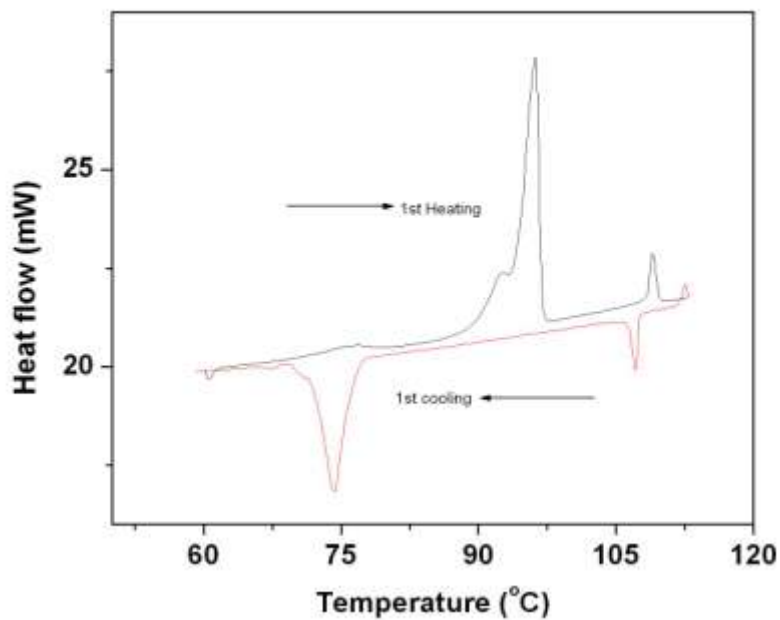
Figure 21. DSC trace of the compound **15e** (scan rate 5 ℃ min^{-1}).
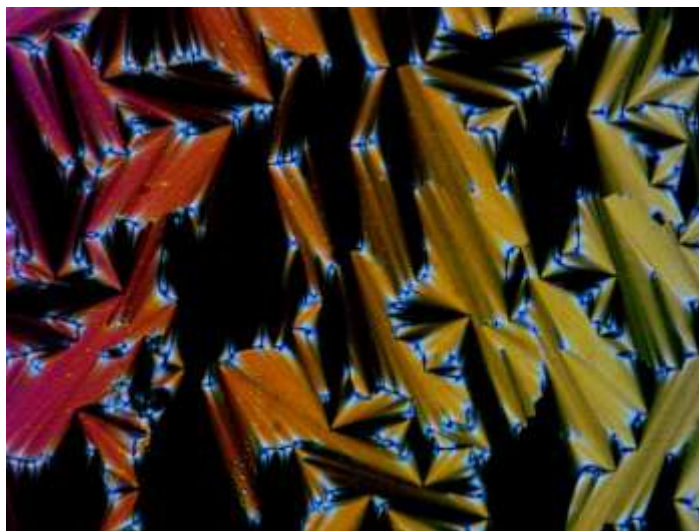
Figure 22. Optical texture of the SmA phase of dimer **15f** obtained on cooling from the isotropic

liquid at 90 ℃ (crossed polarizers, magnification X 200).

Figure 23. The dependence of the transition temperature on the number of atoms (m) in the spacer. For simplicity S atoms have also been treated as carbon atoms. Cr = Crystalline phase; M = Mesophase; N = Nematic phase; I = Isotropic phase; Sm = Smectic phase.
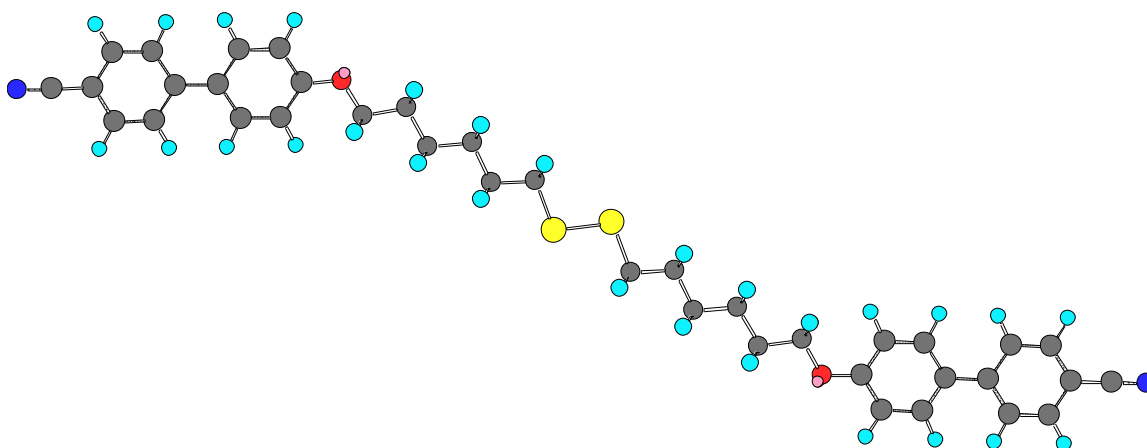
Figure 24. The MM2 energy minimized structure of compound **15a.**

Figure 25. X-ray diffraction patterns obtained for compound **15f** at 96 °C.
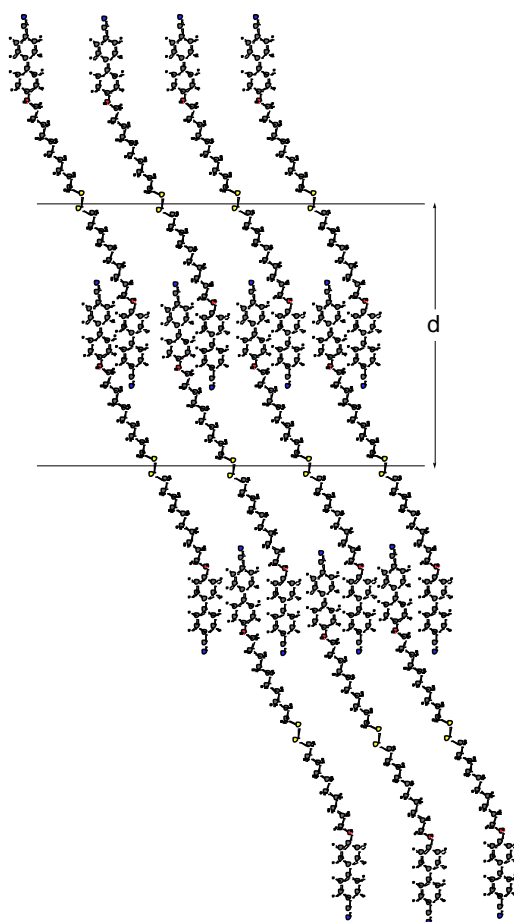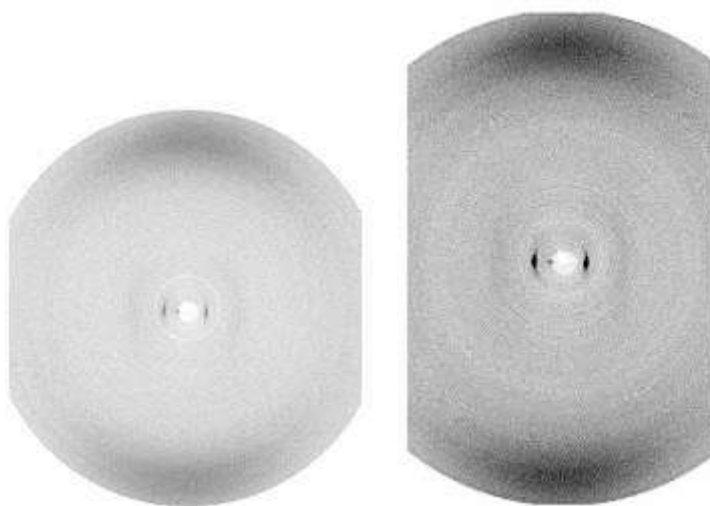

Figure 26. Sketch of the intercalated SmA phase exhibited by **15f**.

Figure 27. X-ray diffraction patterns obtained for compound **15e** at 104 and 90 °C respectively.
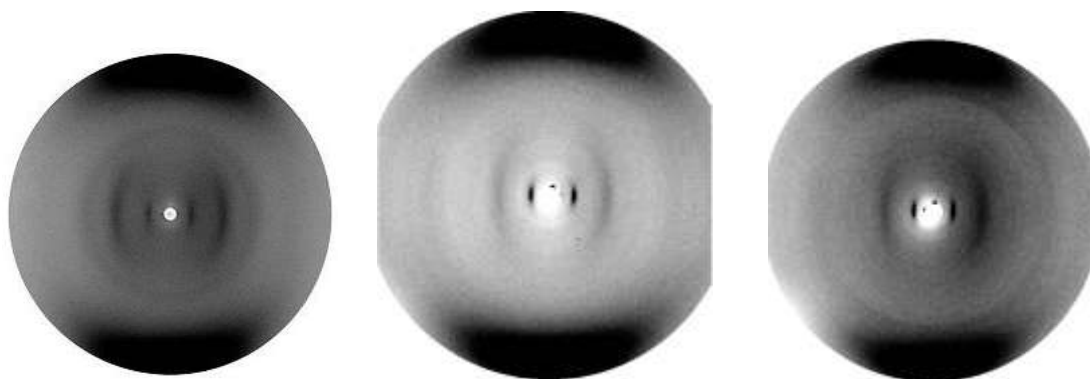

Figure 28. X-ray diffraction patterns obtained for compound **15b**, **15c**, and **15d** at 100, 100 and
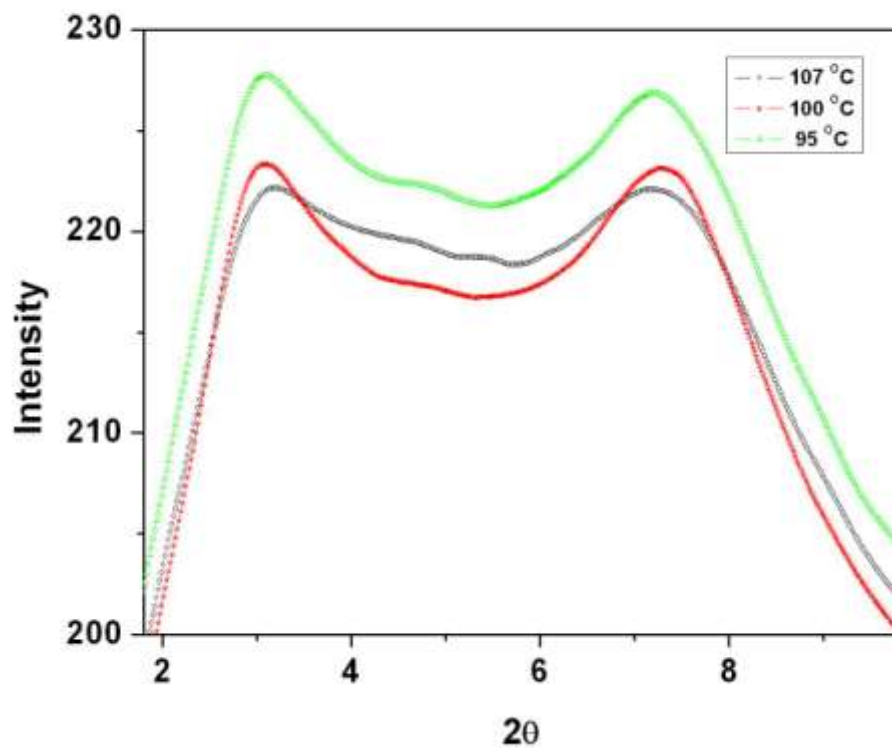
90 °C respectively.

Figure 29. One dimensional Intensity vs. 2θ (deg.) profile for compound **15b** at different
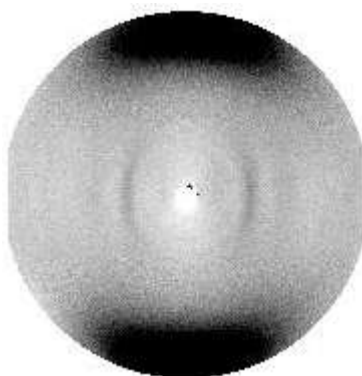
temperatures.

Figure 30. X-ray diffraction patterns obtained for compound **15a** at 100°C.